Efficacy and Prognosis of 3D Printing Technology in Treatment of High-Energy Trans-Syndesmotic Ankle Fracture Dislocation – "Log-Splitter" Injury

Authors' Contribution:
Study Design A
Data Collection B
Statistical Analysis C
Data Interpretation D
Manuscript Preparation E
Literature Search F
Funds Collection G

ABCDEFG 1,2   Yuan-Wei Zhang
BCDE 2   Xin Xiao
CDE 2   Yan Xiao
CDE 2   Xi Chen
EF 3   Su-Li Zhang
ABCDEFG 1   Liang Deng

1 Department of Orthopedics, Jiangxi Provincial People's Hospital Affiliated with Nanchang University, Nanchang, Jiangxi, P.R. China
2 Medical Department, Graduate School, Nanchang University, Nanchang, Jiangxi, P.R. China
3 Department of Surgery, Wujin Hospital Affiliated with Jiangsu University, Changzhou, Jiangsu, P.R. China

Corresponding Author: Liang Deng, e-mail: dengliang001137@163.com
Source of support: Departmental sources

Background:
This study aimed to retrospectively assess the feasibility and efficacy of three-dimensional (3D) printing technology in the treatment of high-energy trans-syndesmotic ankle fracture dislocation – "log-splitter" injury – and to evaluate the efficacy and prognosis.

Material/Methods:
We included 29 patients (17 males and 12 females; mean age, 44.0±13.2 years) with log-splitter injury from June 2011 to December 2016, divided into a routine group (n=13) and a 3D printing group (n=16) according to the surgical method used. Operation time, intraoperative blood loss, fluoroscopy times, fracture union time, functional outcomes based on AOFAS (American Orthopedic Foot and Ankle Society) score, and postoperative complications were observed and recorded.

Results:
Compared with the routine treatment group, 3D printing technology had better safety and efficacy for the treatment of log-splitter injury and the advantages of shorter operation time, less intraoperative blood loss, fewer fluoroscopies needed, and higher rate of good functional outcome ($P<0.001$, $P<0.001$, $P<0.001$, and $P=0.017$, respectively). However, no significant difference was noted in the rate of anatomical reduction, mean AOFAS score at the last follow-up (mean time, 19.9±2.8 months), or postoperative complications between the 2 groups ($P=0.370$, $P=0.156$, and $P=0.485$, respectively).

Conclusions:
Surgery assisted by 3D printing technology to treat log-splitter injury is feasible and effective, and may be a good optional approach to formulate a reasonable personalized surgical plan and to optimize the outcomes.

MeSH Keywords:
Ankle Fractures • Ankle Injuries • Ankle Joint • Complement C3d

Full-text PDF:
https://www.medscimonit.com/abstract/index/idArt/916884

📄 3617   🗐 4   📊 5   📖 32

Background

The ankle joint is one of most significant weight-bearing joints in the entire human body, and its fracture accounts for 3.92% of all fractures [1,2]. Approximately 11% to 20% of ankle fractures are accompanied by distal tibiofibular syndesmotic injury, which greatly affects ankle joint stability of [3–5]. However, as an newly proposed type of high-energy ankle fracture and dislocation [6,7], the injury mechanism of log-splitter injury may be described as similar to an inverted log-splitter wedge, which is a kind of industrial device used for splitting firewood (Figure 1). Under the multi-force action dominated by vertical axial force, the talus is simulated as a sharp wedge embedded into the distal tibiofibular syndesmosis, leading to distal syndesmotic disruption and displacement, as well as injury to the surrounding soft tissue [7].

Open reduction and internal fixation (ORIF) is performed by exposing the fracture site, repairing and resetting the fracture end, and selecting different specifications of internal fixation to maintain the position after reduction, and is considered as the standard therapy for ankle fracture and dislocation [8]. However, recent related studies have reported that the incidence of complications such as poor wound healing, wound infection, and lower-extremity venous thrombosis after ORIF is high [9]. To achieve better efficacy and prognosis, ORIF needs to be more precise and personalized. With the rapid development of 3D printing technology in the field of digital orthopedics, an intuitive and physical model can be reconstructed based on computed tomography (CT) scan data by printing layer-by-layer after the processes of virtual reset and simulated fixation, which helps surgeons understand the location and displacement of fractures, as well as formulating an optimal preoperative plan and conducting surgical strategy simulation [10,11].

Hence, in order to further clarify the feasibility and efficiency of 3D printing assisted surgery for log-splitter injury, this retrospective study compared the traditional surgery with 3D printing surgery in the treatment of log-splitter injury, and evaluated the prognosis.

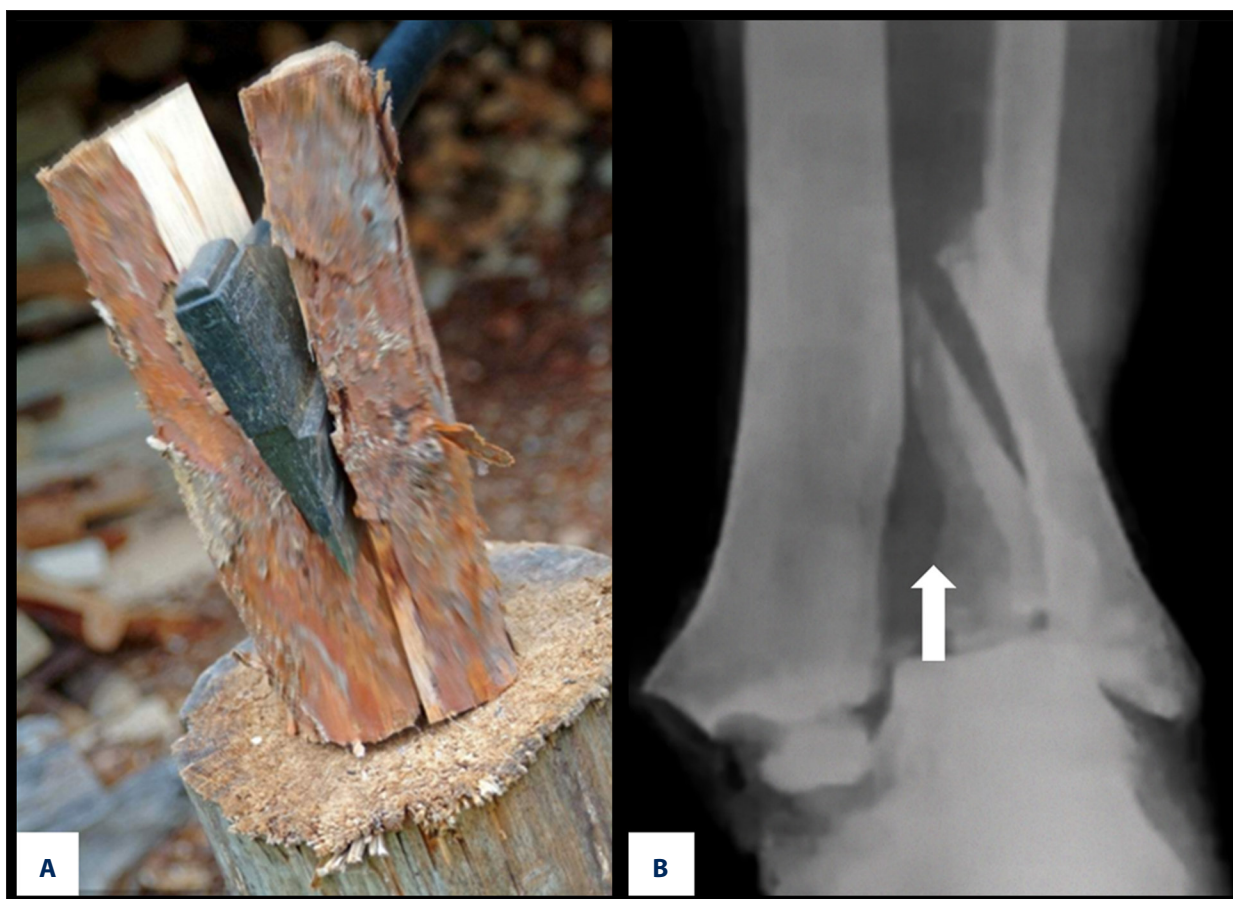**Figure 1.** Schematic diagrams of log-splitter injury. (**A**) The industrial wedge for splitting firewood is similar to log-splitter injury in morphology, which is vividly described as the "log-splitter injury". (**B**) The talus is simulated as a sharp wedge embedded into (along with the direction of arrow) the distal tibiofibular syndesmosis, leading to distal syndesmotic disruption and displacement.

Material and Methods

Diagnostic criteria and clinical classification

Log-splitter injury was described as an ankle fracture and dislocation caused by the vertical axial force and possibly combined rotational force, including the distal tibiofibular syndesmotic disruption and displacement, as well as the surrounding soft tissue compromise [6,7]. Therein, distal tibiofibular syndesmotic disruption and displacement were diagnosed referring to Amendola et al. [12] on the basis of the normal anatomical relationship of distal tibiofibular syndesmosis on X-rays: (1) the space of distal tibiofibular was less than or equal to 6 mm on anteroposterior position or ankle mortise view; (2) the overlap of tibiofibular on anteroposterior position was greater than 6 mm or 42% of the fibula width; and (3) the overlap of tibiofibular on ankle mortise view was greater than 1 mm. Values beyond any of these ranges were regarded as syndesmotic disruption or displacement.

In addition, Wang et al. [6] also classified log-splitter injury into typical and atypical types according to the degree of talus embedded into the distal tibiofibular syndesmosis. In the typical type, the talus is usually completely embedded into the distal tibiofibular syndesmosis caused by vertical axial force, with or without the "Platford" and talus fracture. In the atypical type, the talus is usually incompletely or partially embedded into the distal tibiofibular syndesmosis caused by the rotational force, without "Platford" and talus fracture.

Patients

This retrospective study reviewed a total of 29 patients (17 males and 12 females) who were diagnosed with log-splitter injury according to the above criteria, and who were admitted to Jiangxi Provincial People's Hospital affiliated with Nanchang University from June 2011 to December 2016. As 3 patients in the routine group were followed up for less than 12 months, patients were enrolled in the routine group (n=13) and 3D printing group (n=16) by random number table method after admission, and treated according to the different surgical methods. Moreover, on the basis of previous research standards by Bible and Wang [6,7], the inclusion criteria included: (1) age range of 18–75 years; (2) fresh injuries (within 2 weeks from injury); and (3) at least 12 months of follow-up. The exclusion criteria included: (1) old and pathological fractures; (2) patients with severe cardiovascular diseases, liver or kidney disease, or central nervous system diseases who could not tolerate the surgery; and (3) patients who were lost to follow-up or were followed up for less than 12 months. This study was approved by the Institutional Review Board of Jiangxi Provincial People's Hospital affiliated with Nanchang University.

Printing the 3D models

We collected CT scan data of 16 patients with log-splitter injury from the dual-source 64-slice spiral CT system (SIEMENS, Germany) in our hospital. The scan parameters were 120 KV voltage and 0.625 mm pitch. All original CT data were stored in Digital Imaging and Communications in Medicine (DICOM) format and imported into Mimics 19.0 software (Materialise, Leuven, Belgium) for 3D reconstruction, and the structural features of talus, broken bones, and peri-ankle bones were accurately separated by functions of Thresholding and Split Mask. After Boolean operation, the restored fracture blocks were spliced together, and the noise reduction and smoothing were further performed. The fracture blocks were then virtually reset by the Move and Rotate operations. The design data was then imported into the 3D printing software (Cura 15.02) in STL format. After forming the 3D digital model, the data were saved in Gcode format and exported to a 3D printer (Waston Med, Inc., Changzhou, China), and a 1: 1 physical model of the injured ankle joint was fabricated with photosensitive resin.

Surgery simulation

With the assistance of a 3D-printed log-splitter injury physical model, surgeons were able to simulate the extracorporeal operation in advance. In this process, surgeons can perform the simulated resets and fixations on models, and attach the appropriate plates and screws with desired length, direction, and position to the models. These preselected and prefabricated plates and screws were then sterilized and stored for later actual surgery. The fracture structure features in the 3D-printed model were clear, which contributes to their usefulness as a reference for anatomical reduction during actual surgery.

Operative procedures

All surgical procedures were performed by senior surgeons in the same treatment team. Under general or epidural anesthesia, patients were placed into supine position and a pneumatic tourniquet was used at the root of the thigh to block the blood circulation. A suitable surgical approach to achieve satisfactory reduction was selected according to the different injury patterns. After incising the skin, the subcutaneous tissues were bluntly dissected to fully expose the fracture end. The operation first fixes the fibula or lateral malleolus, and a 3.5-mm locking compression plate (LCP) of varying length and the cortical locking screws of different specifications (Weigao Med, Inc., Weihai, China) were selected as usual to restore the fibula length and adjust the limb force line. Then, the possibly combined Platford fracture of distal tibia, Chaput fracture of anterolateral tibia, Volkmann fracture of posterior ankle, and the anterior or medial malleolus ankle fracture were reduced and fixed. Afterwards, according to the measurement results of

This work is licensed under Creative Common Attribution-NonCommercial-NoDerivatives 4.0 International (CC BY-NC-ND 4.0)

4235

Indexed in: [Current Contents/Clinical Medicine] [SCI Expanded] [ISI Alerting System] [ISI Journals Master List] [Index Medicus/MEDLINE] [EMBASE/Excerpta Medica] [Chemical Abstracts/CAS]

the hook test, the stability of reduced ankle joint was judged, the distal tibiofibular syndesmosis was selectively fixed, and the deltoid ligament or distal anteroposterior tibiofibular ligament were repaired. In the 3D printing group, the insertion of plates and screws directly referred to the results of preoperative 3D-printed model simulation. However, the selection and insertion of plates and screws in the routine group were determined only by intraoperative measurements and fluoroscopy results. After the reduction and fixation were evaluated by the C-shaped X-ray, the incision was closed layer-by-layer with 2/0 absorbable sutures, as usual.

Postoperative management

There was no significant significance in postoperative management of patients between the 2 groups. The antibiotics were applied within 2 days postoperatively to prevent infections; the injured limbs were raised to alleviate the swelling around the incision; patients were encouraged to take functional exercises as early as possible to prevent the ankle joint stiffness; weight-bearing was avoided within 3 months, until the imaging examination confirmed the formation of continuous callus at the fracture end, patients were guided to partly weight-bearing and gradually transitioned to complete weight-bearing. In addition, according to the previous study by Miller et al. and Hamid et al. [13,14], the distal tibiofibular syndesmotic screw was supposed to be removed 12–14 weeks postoperatively to avoid complications such as limited joint motion, joint stiffness, and pain above the distal tibiofibular syndesmosis after weight-bearing.

Parameters assessment

The operation time, intraoperative blood loss, fluoroscopy times, fracture union time, and postoperative complications of all patients were observed and recorded. The range of ankle joint motion, including dorsal expansion, plantarflexion, inversion, and eversion, were also assessed at follow-ups. Moreover, preoperative and postoperative tibiofibular widths were measured based on the axial CT of the ankle joint. On the basis of anteroposterior X-rays of the ankle joint, the fracture reduction was evaluated by scoring according to the Burwell-Charnley radiographic criteria [15]. During the last follow-up, the ankle functional outcomes were assessed by American Orthopedic Foot and Ankle Society (AOFAS) ankle-hind foot score [16]. In the 100-point AOFAS scoring system, a score ≥90 is regarded as excellent, 75–89 as good, 50–74 as fair, <50 as poor.

Statistical analysis

Data were statistically analyzed by SPSS 22.0 software (SPSS, Inc., Chicago, USA) and are presented as count (percentage) or mean ± standard deviation (SD). The t test, chi-squared test, and Fisher exact test were used to analyze the data. Different parameters measured between 2 groups were assessed with the independent t test for continuous variables, and chi-square test or Fisher exact test for categorical variables. A P value <0.05 was accepted as statistically significant.

Results

Patient characteristics

Demographic data and injury characteristics of patients in the 2 groups are shown in Table 1. The routine group included 8 males and 5 females and the 3D printing group included 9 males and 7 females. The mean age of patients in the routine group was 43.3±13.9 years and in 44.5±13.5 years in the 3D printing group. Regarding the causes of injury, the most common in the 2 groups was falling from a height (7/13 versus 9/16). In the routine group, the injuries were on the left in 8 patients and on the right in 5. In the 3D printing group, the injuries were on the left in 6 patients and on the right in 10. Based on the clinical classification of log-splitter injury [6], the routine group had 9 patients with typical injury (mainly vertical axial force), and 4 patients with atypical injury (mainly rotational force). The 3D printing group had 10 patients with typical injury and 6 patients with atypical injury. Moreover, according to AO fracture classification [17,18], there were 2 patients with type 44A fracture, 3 patients with type 44B fracture, and 8 patients with type 44C fracture in the routine group. The 3D printing group included 3 patients with type 44A fracture, 4 patients with type 44B fracture, and 9 patients with type 44C fracture. On the basis of AO soft tissue injury grading [19], there were 8 patients with grade IC1, 3 patients with grade IC2, and 2 patients with grade IC3 in the routine group, and there were10 patients with grade IC1, 4 patients with grade IC2, and 2 patients with grade IC3 in the 3D printing group. Time from injury to operation in the routine group was 7.1±2.9 days and it was 7.4±2.7 days in the 3D printing group. In the routine group, there were 3 patients with tibial Platford fracture, 2 patients with Tillaux-Chaput avulsion fracture, and 3 patients with Volkmann fracture. In the 3D printing group, 4 patients had tibial Platford fracture, 3 patients had Tillaux-Chaput avulsion fracture, and 2 patients had Volkmann fracture. Maisonneuve fracture was not observed in either group. The comparison of preoperative data between the 2 groups revealed no significant difference in age, sex, causes of injury, injury side, injury type, fracture classification, soft tissue injury grading, time from injury to operation, and the associated fractures (P>0.05 for all).

Clinical data

There was a significant difference in operation time between the 3D printing group (107.8±10.2 min) and the routine group (124.5±11.5 min, P<0.001). The intraoperative blood loss in

Table 1. Comparison of demographic data and injury characteristics between the 2 groups.

Characteristics	Routine group (n=13)		3D printing group (n=16)		P value
Mean age (range), years	43.3±13.9 (21–65)		44.5±13.5 (20–67)		0.867
Gender					0.965
Male	8		9		
Female	5		7		
Causes of injury, n (%)					0.774
Falling from height	7	(53.8)	9	(56.2)	
Traffic accidents	3	(23.1)	3	(18.8)	
Sprain	1	(7.7)	1	(6.2)	
Crashes by heavy objects	2	(15.4)	3	(18.8)	
Injury side, n (%)					0.183
Left	8	(61.5)	6	(37.5)	
Right	5	(38.5)	10	(62.5)	
Injury type, n (%)					0.497
Typical injury	9	(69.2)	10	(62.5)	
Atypical injury	4	(30.8)	6	(37.5)	
AO/OTA type, n (%)					0.879
44A	2	(15.4)	3	(18.8)	
44B	3	(23.1)	4	(25.0)	
44C	8	(61.5)	9	(56.2)	
Soft tissue injury grading, n (%)					0.985
IC1	8	(61.5)	10	(62.5)	
IC2	3	(23.1)	4	(25.0)	
IC3	2	(15.4)	2	(12.5)	
Time from injury to operation, days	7.1±2.9		7.4±2.7		0.711
Associated fractures, n (%)					
Tibial Platford fracture	3	(23.1)	4	(25.0)	0.678
Tillaux-Chaput avulsion fracture	2	(15.4)	3	(18.8)	0.276
Volkmann fracture	3	(23.1)	2	(12.5)	0.699
Maisonneuve fracture	0		0		–

the 3D printing group (99.6±19.3 ml) was significantly less than that of the routine group (133.7±26.2 ml, $P<0.001$). Moreover, the number of times fluoroscopy was used during the operation in the 3D printing group (7.3±2.7 times) was also significantly lower compared with the routine group (11.7±2.4 times, $P<0.001$). As for fracture union time, there was no significant difference between the 3D printing group (5.1±1.2 months) and routine group (5.2±1.3 months, $P=0.550$). According to the Burwell-Charnley grading criteria [15], 13 patients in the 3D printing group obtained anatomical reduction, 2 patients obtained fair prognosis, and 1 patient obtained poor prognosis, while in the routine group, 9 patients obtained anatomical reduction, 3 patients obtained fair prognosis, and 1 patient obtained poor prognosis. There was no significant difference in fracture reduction between the 2 groups ($P=0.183$), and there was no significant difference in the rate of anatomical reduction (69.2% versus 81.3%, $P=0.370$). The results of clinical data are summarized in Table 2.

Table 2. Comparison of clinical data between the 2 groups.

Clinical data	Routine group (n=13)	3D printing group (n=16)	P value
Operation time, min	124.5±11.5	107.8±10.2	<0.001
Intraoperative blood loss, ml	133.7±26.2	99.6±19.3	<0.001
Fluoroscopy times, n	11.7±2.4	7.3±2.7	<0.001
Fracture union time, month	5.2±1.3	5.1±1.2	0.550
Fracture reduction	–	–	0.183
Anatomic, n	9	13	0.250
Fair, n	3	2	0.452*
Poor, n	1	1	0.575*
Rate of anatomic reduction, %	69.2	81.3	0.370

Parameters were assessed with *t* test for continuous variables; * *P* value for continuity-corrected chi-squared test.

Table 3. Comparison of postoperative functional outcomes between the 2 groups.

Outcomes	Routine group (n=13)	3D printing group (n=16)	P value
Follow-up time, months	19.5±2.9	20.2±2.8	0.408
Preoperative tibiofibular width, mm	14.12±2.77	14.90±2.70	0.660
Postoperative tibiofibular width, mm	5.26±0.92	5.19±0.67	0.583
Range of ankle motion, °			
Dorsal expansion	23.5±3.8	24.3±3.9	0.313
Plantarflexion	26.7±3.4	27.9±2.8	0.291
Eversion	27.6±3.1	28.4±2.6	0.364
AOFAS score at last follow-up	74.8±9.3	75.5±8.5	0.156
Excellent, n (%)	0	0	–
Good, n (%)	10 (76.9)	14 (87.5)	0.602
Fair, n (%)	2 (15.4)	1 (6.25)	0.117*
Poor, n (%)	1 (7.7)	1 (6.25)	0.656*
Rate of good outcome,%	76.9	87.5	0.017

Parameters were assessed with *t* test for continuous variables; * *P* value for continuity-corrected chi-squared test; AOFAS – American Orthopedic Foot and Ankle Society.

Postoperative functional outcomes

All patients were successfully followed up for more than 12 months. There was no significant difference in follow-up time between the 3D printing group (20.2±2.8 months) and routine group (19.5±2.9 months, *P*=0.408). Average preoperative tibiofibular width in the 3D printing group was 14.90±2.70 mm, and in the routine group it was 14.12±2.77 mm (*P*=0.660). After complete weight-bearing, the width in the 2 groups decreased to 5.19±0.67 mm and 5.26±0.92 mm, respectively, which was not significantly different (*P*=0.583). Furthermore, the ankle functional outcomes of patients in the 2 groups were all improved compared with the initial situation. As represented in Table 3, the motion of dorsal expansion was 24.3±3.9° in the 3D printing group and 23.5±3.8° in the routine group (*P*=0.313). The motion of plantar flexion was 27.9±2.8° in the 3D printing group and 26.7± 3.4° in the routine group was (*P*=0.291). The motion of inversion was 25.7±3.8° in the 3D printing group and 24.4±3.5° in the routine group (*P*=0.186). The motion of eversion was 28.4±2.6° in the 3D printing group and 27.6±3.1° in the routine group (*P*=0.364). There was no significant difference in ankle motions between the 2 groups. In addition,

Table 4. Comparison of complications between the 2 groups.

Complications	Routine group (n=13)		3D printing group (n=16)		P value
Superficial infection	1	(10.5)	1	(8.3)	1.000*
Deep infection	0		0		–
Posttraumatic arthritis	0		0		–
Delayed fracture union	1	(10.5)	2	(12.5)	1.000*
Malunion	1	(5.3)	0		1.000*
Nonunion	0		0		–
Total	3	(23.1)	3	(18.8)	0.485

Values are expressed as, *n* (%); * *P* value for Fisher's exact test.

Expected values	Routine group (*n*=13)	3D printing group (*n*=16)
Superficial infection	0.90	1.10
Deep infection	0	0
Post-traumatic arthritis	0	0
Delayed fracture union	1.34	1.66
Malunion	0.45	0.55
Nonunion	0	0
Total	–	–

the mean AOFAS score at the last follow-up in the 3D printing group was 75.5±8.5, with 10 patients scored as good, 2 as fair, and 1 as poor, while that of the routine group was 74.8±9.3, with 14 patients scored as good, 1 as fair, and 1 as poor. There was no significant difference in AOFAS score between the 2 groups (*P*=0.156). However, compared with the routine group (76.9%), the 3D printing group (87.5%, *P*=0.017) exhibited a higher rate of good functional outcome.

Postoperative complications

There was 1 patient in each group with superficial infection, which were successfully controlled by antibiotics and regular dressing. In the 3D printing group, there were 2 patients with delayed fracture union, while the routine group has 1 such patient. However, all of them healed after functional exercises and enhanced weight-bearing within 9 months after the operation. No other complications such as malunion, nonunion, and deep infection were found in the remaining patients. As summarized in Table 4, the total complication rate of the 3D printing group was 18.8% (3/16) and in the routine group it was 23.1% (3/13), with no significant difference between groups (*P*=0.485).

Typical case

A male, 29 years old, falling from a height, was diagnosed with log-splitter injury and selected as the typical case.

The preoperative X-ray and CT scan of injured ankle joint are shown in Figure 2. Based on his CT scan data, the functions of Thresholding and Split Mask in Mimics 19.0 software were used to clearly exhibit the characteristics of the injured ankle, and the outcome of virtual reset is presented in Figure 3. The 1: 1 physical model of injured ankle was then fabricated and a simulated operation was performed *in vitro* (Figure 4). Afterwards, the subsequent actual surgery was guided by the simulated operation. Postoperative X-rays suggested the reduction and fixation were satisfactory (Figure 5). To avoid complications such as limited joint motion, joint stiffness, and pain above the distal tibiofibular syndesmosis, the distal tibiofibular syndesmotic screw was removed 12 weeks postoperatively [13,20]. During follow-up over the next 20 months, he was generally in good condition and the ankle function recovered well.

Discussion

The conception of log-splitter injury was first proposed by Bible et al. in 2014 [7], which represents an exceptional type of high-energy transsyndesmotic ankle fracture dislocation. With the combination of vertical axial force and possible rotational force, the injury energy is very high and often results in distal syndesmotic disruption and displacement, as well as the damage to the surrounding soft tissue [6,7]. The mechanism of log-splitter injury is complicated, and can be divided
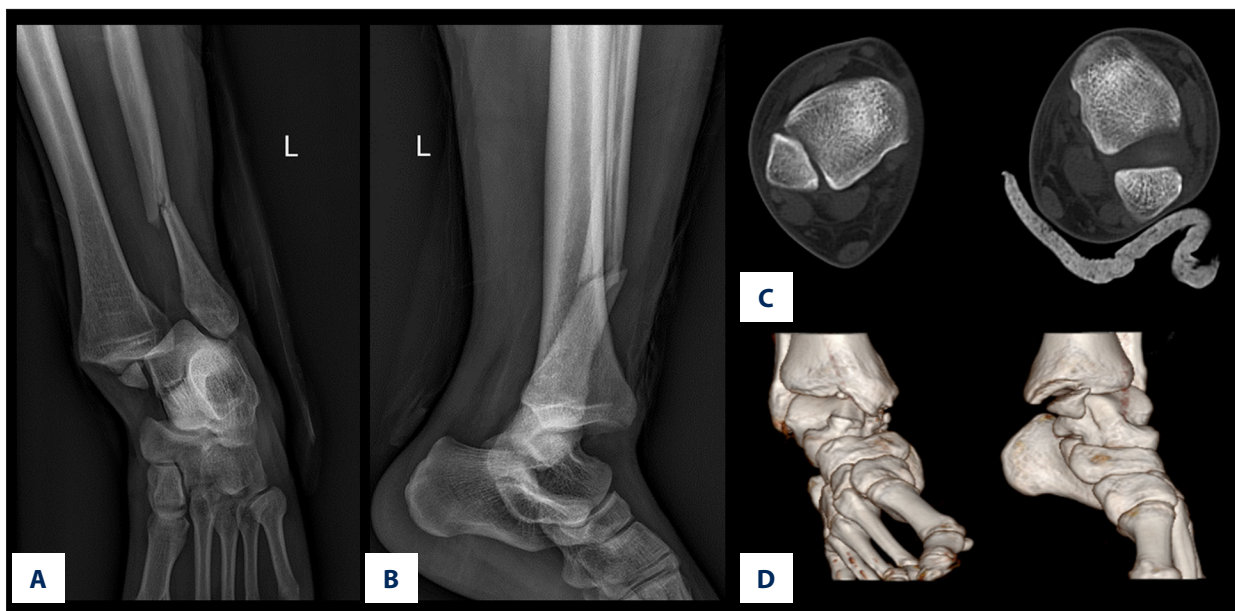
Figure 2. Preoperative radiographs of log-splitter injury. (**A**) Anteroposterior X-ray of injured ankle joint. (**B**) Lateral X-ray of injured ankle joint. (**C**) Axial CT image of bilateral ankle joints. (**D**) CT three-dimensional reconstruction of bilateral ankle joints
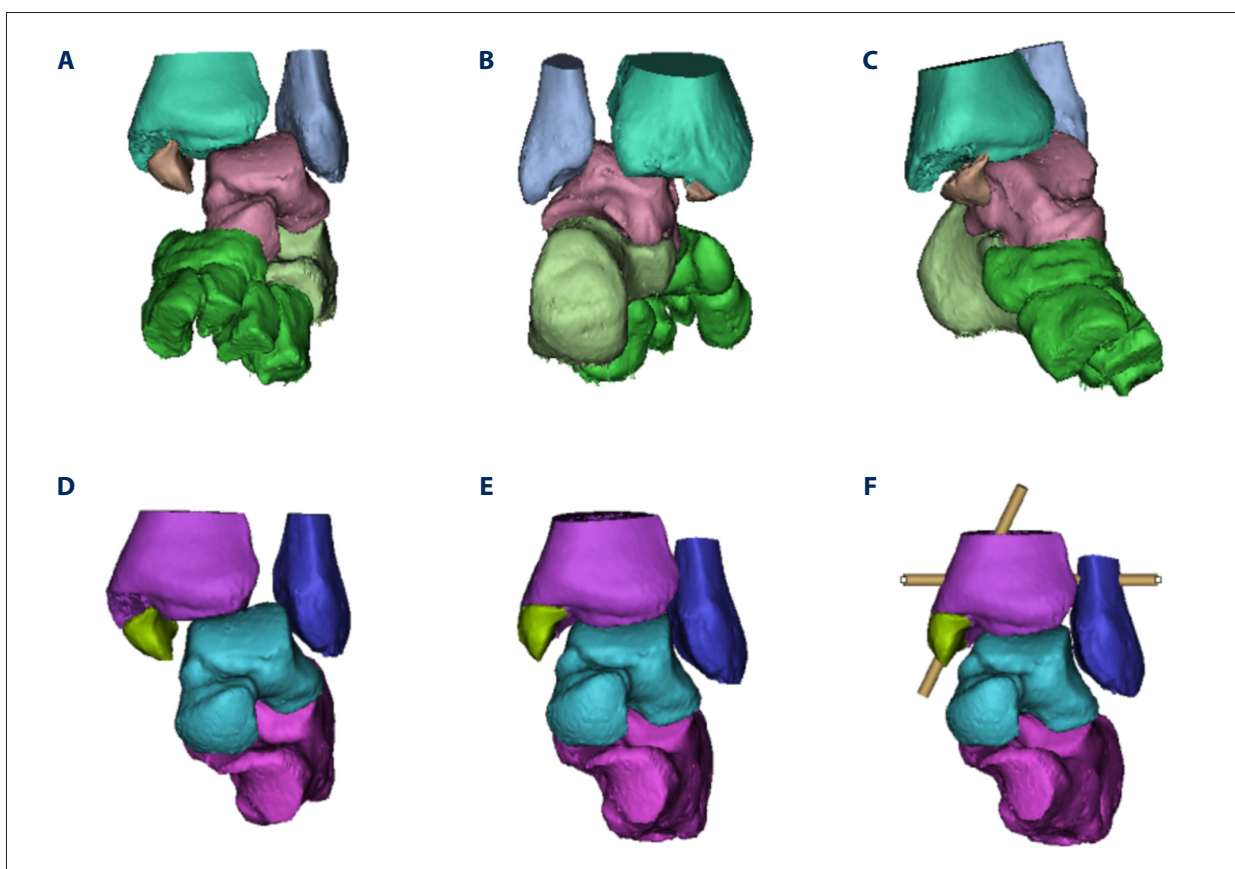

Figure 3. The reconstruction, simulated reduction, and fixation of log-splitter injury in Mimics 19.0 software. (**A**) Anterior view of reconstructed model. (**B**) Posterior view of reconstructed model. (**C**) Lateral view of reconstructed model. (**D**) Reconstructed model after the operations of noise reduction and smoothing. (**E**) Reconstructed model after virtual reset. (**F**) Reconstructed model after virtual fixation
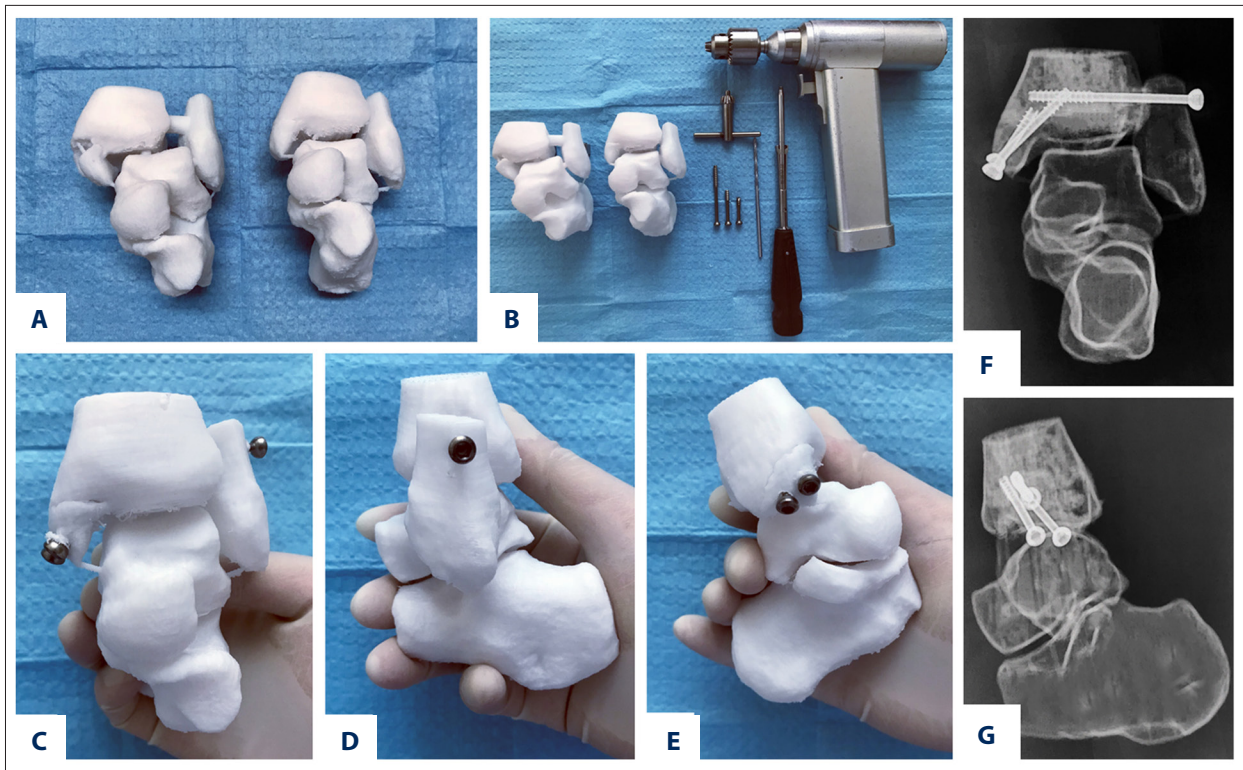
Figure 4. Simulated extracorporeal operation prior to the actual surgery. (**A**) 3D printed models before and after reset. (B) Preparation of simulated operation. (**C–E**) Simulating the operation on the model (**C:** Anterior view, **D:** Left lateral view, **E:** Right lateral view). (**F, G**) X-rays after simulated operation (**F:** Anteroposterior view, **G:** Lateral view).

into typical type and atypical type only according to the degree of talus embedded into the distal tibiofibular syndesmosis [6]. The current therapies of log-splitter injury are single and indefinite, mainly relying on ORIF and the repair of distal tibiofibular syndesmosis, with a certain disability rate, varying surgical efficacy, and labile complication rate.

Hence, we retrospectively compared the efficacy and prognosis of conventional surgery versus surgery assisted by 3D printing technology in the treatment of log-splitter injury. In the 3D printing group, the anatomical relationship of the injured ankle can be more clearly and intuitively understood on the basis of the 3D printed model, which effectively assists surgeons in determining the fracture classification and distribution of broken bones [21,22], and the collapse and comminution of the articular surface can be also examined. Thus, whether bone grafting is needed or the amount of bone grafting needed can be accurately assessed in this process, which contributes to formulating a reasonable personalized surgical plan and optimizing the outcomes [23].

With the simulated extracorporeal operation on models in the 3D printing group, the plates and screws were precisely preselected and prefabricated, and the position and direction of screws insertion were marked out. The operation time, intraoperative

blood loss, and fluoroscopy times in the 3D printing group were significantly less than those in the routine group, and obtained a higher rate of good functional outcome. The results were similar to the previous studies by Zheng et al. and Bai et al. [24,25]. The AOFAS score for our cohort of log-splitter injury in the 3D printing group was 75.5±8.5 at the last follow-up, which is a little higher than that of the study by Bible et al. (67.0±26.8) [7]. In addition, with the assistance of 3D printing technology, the radiation exposure of surgeons and patients can be effectively reduced, as well as the incidence of potential risks during surgery and anesthesia [26–30]. In addition, the 3D printed model allows to explain detailed the operation plan and related risks to patients and their families, which enhances doctor-patient communication and enables patients to have an intuitive understanding of the surgery [24].

However, despite the apparent advantages of 3D printing technology, it is necessary to clearly recognize that there are still some shortcomings. Firstly, no significant difference was noted in mean AOFAS score at the last follow-up between the 2 groups (75.5±8.5 versus 74.8±9.3, P=0.156). Secondly, there was no significant difference in the total complication rate between the 2 groups (18.8% versus 23.1%, P=0.485), which indicates that the 3D printing technology is not superior to preventing complications. The above results were similar to
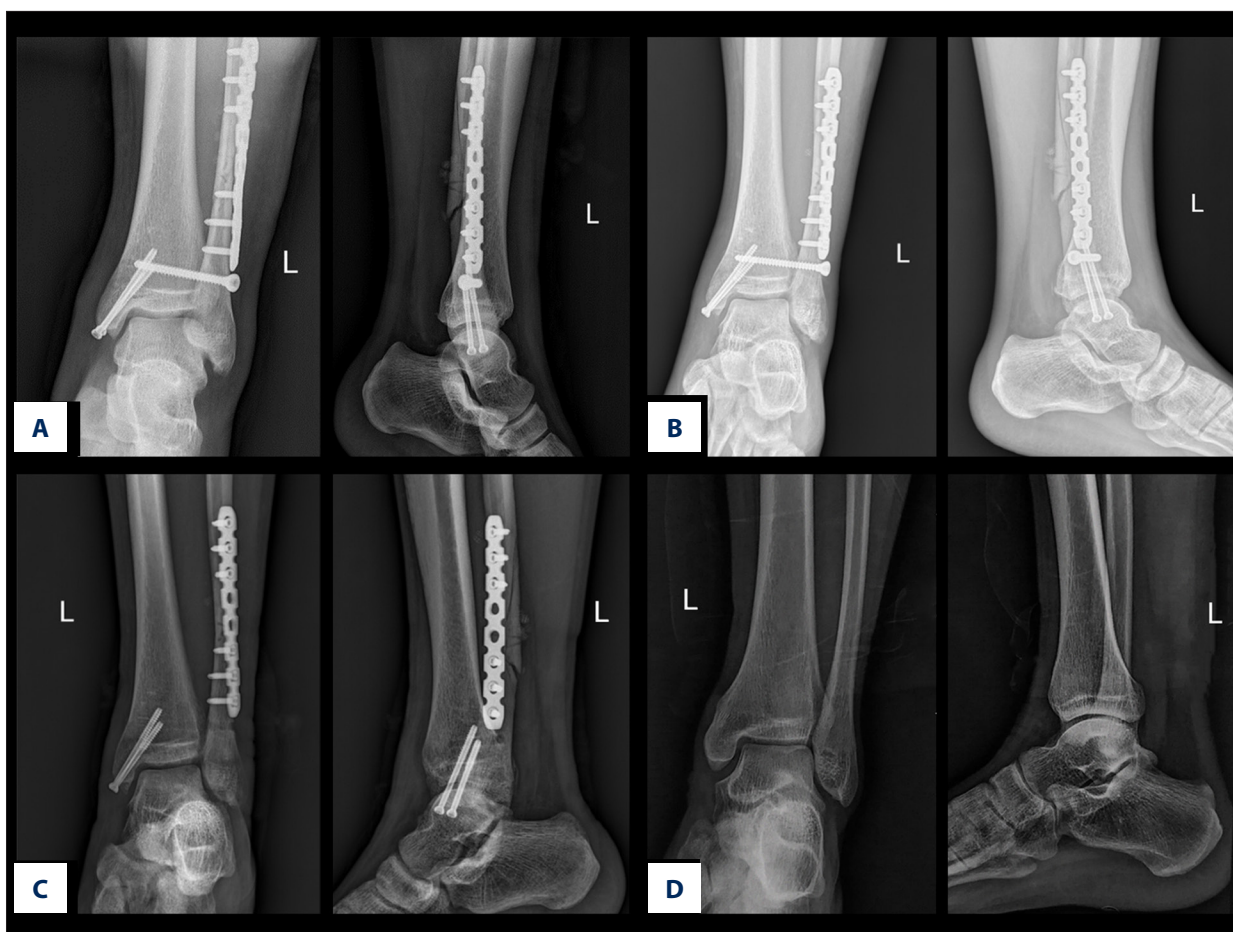
Figure 5. Postoperative radiographs after the surgery. (**A**) Anteroposterior and lateral X-ray after surgery. (**B**) Anteroposterior and lateral X-ray at 1-month follow-up. (**C**) The distal tibiofibular syndesmotic screw was removed 12 weeks postoperatively. (**D**) Anteroposterior and lateral X-ray at 20-month follow-up (after internal fixation removal).

the study reported by Wang et al. [31]. Thirdly, there was no significant difference in the rate of anatomical reduction between the 3D printing group and routine group (81.3% versus 69.2%, *P*=0.370), which was not consistent with that of the research by Zheng et al. applying the 3D printing technology to the pilon fracture (91.1% versus 75%, *P*=0.040) [24]. This might be related to the high-energy injury caused by multi-force violence of log-splitter injury [6,7], whose traumatic energy is greater than that of the Pilon fracture to a certain extent, as demonstrated by the fact that none of the patients had an excellent score (AOFAS score ≥90) in this study. In addition, 3D printing technology is based on CT scan data, and only has a clear image of the skeleton, which lacks the information of adjacent blood vessels, nerves, ligaments, and other soft tissues [24,32]. With the current 3D printing equipment, operation costs and printing materials are relatively expensive, which limits its clinical applications. The whole process from CT scan to printing out the physical model and simulated operation is also time-consuming, taking about 3–5 days, and is not suitable for emergency surgery [24].

Ultimately, certain limitations in this study should also be recognized and addressed. This study is only a retrospective analysis of cases, with a relatively small sample size. To further verify the efficacy and prognosis of surgery assisted by 3D printing technology for log-splitter injury, further prospectively studies with larger samples of high-quality cases from multiple research centers are needed. In addition, as this study was not a prospective, randomized control trial, we did not compare log-splitter injury with other types of ankle fractures, which should be addressed in future studies.

Conclusions

Log-splitter injury represents an exceptional type of high-energy transsyndesmotic ankle fracture dislocation. 3D printing technology is equipped with both safety and efficiency for the treatment of log-splitter injury and has the advantages of shorter operation time, less intraoperative blood loss, fewer fluoroscopy times, and higher rate of good functional outcome

compared with the routine group. Surgery assisted by 3D printing technology to treat log-splitter injury is feasible and effective, and may be an optional approach to formulate a reasonable personalized surgical plan and optimize outcomes.

Competing interests

None.

References:

1. Xu HL, Li X, Zhang DY et al: A retrospective study of posterior malleolus fractures. Int Orthop, 2012; 36(9): 1929–36

2. Salai M, Dudkiewicz I, Novikov I et al: The epidemic of ankle fractures in the elderly – is surgical treatment warranted? Arch Orthop Trauma Surg, 2000; 120(9): 511–13

3. McCollum GA, van den Bekerom MP, Kerkhoffs GM et al: Syndesmosis and deltoid ligament injuries in the athlete. Knee Surg Sports Traumatol Arthrosc, 2013; 21(6): 1328–37

4. Weening B, Bhandari M: Predictors of functional outcome following transsyndesmotic screw fixation of ankle fractures. J Orthop Trauma, 2005; 19(2): 102–8

5. Fallat L, Grimm DJ, Saracco JA: Sprained ankle syndrome: Prevalence and analysis of 639 acute injuries. J Foot Ankle Surg, 1998; 37(4): 280–85

6. Wang Z, Tang X, Li S et al: Treatment and outcome prognosis of patients with high-energy transsyndesmotic ankle fracture dislocation-the "Logsplitter" injury. J Orthop Surg Res, 2017; 12(1): 3

7. Bible JE, Sivasubramaniam PG, Jahangir AA et al: High-energy transsyndesmotic ankle fracture dislocation – the "Logsplitter" injury. J Orthop Trauma, 2014; 28(4): 200–4

8. Hak DJ, Lee M, Gotham DR: Influence of prior fasciotomy on infection after open reduction and internal fixation of tibial plateau fractures. J Trauma, 2010; 69(4): 886–88

9. Miller AG, Margules A, Raikin SM: Risk factors for wound complications after ankle fracture surgery. J Bone Joint Surg Am, 2012; 94(22): 2047–52

10. Xu R, Wang Z, Ma T, Ren Z, Jin H: Effect of 3D printing individualized ankle-foot orthosis on plantar biomechanics and pain in patients with plantar fasciitis: A randomized controlled trial. Med Sci Monit, 2019; 25: 1392–400

11. Jeong HS, Park KJ, Kil KM et al: Minimally invasive plate osteosynthesis using 3D printing for shaft fractures of clavicles: Technical note. Arch Orthop Trauma Surg, 2014; 134(11): 1551–55

12. Amendola A, Williams G, Foster D: Evidence-based approach to treatment of acute traumatic syndesmosis (high ankle) sprains. Sports Med Arthrosc Rev, 2006; 14(4): 232–36

13. Miller AN, Paul O, Boraiah S et al: Functional outcomes after syndesmotic screw fixation and removal. J Orthop Trauma, 2010; 24(1): 12–16

14. Hamid N, Loeffler BJ, Braddy W et al: Outcome after fixation of ankle fractures with an injury to the syndesmosis: The effect of the syndesmosis screw. J Bone Joint Surg Br, 2009; 91(8): 1069–73

15. Burwell HN, Charnley AD: The treatment of displaced fractures at the ankle by rigid internal fixation and early joint movement. J Bone Joint Surg Br, 1965, 47(4): 634–60

16. Lee MS, Maker JM: Revision of failed flatfoot surgery. Clin Podiatr Med Surg, 2009; 26(1): 47–58

17. Juto H, Nilsson H, Morberg P: Epidemiology of adult ankle fractures: 1756 cases identified in Norrbotten County during 2009–2013 and classified according to AO/OTA. BMC Musculoskelet Disord, 2018; 19(1): 441

18. Juto H, Moller M, Wennergren D et al: Substantial accuracy of fracture classification in the Swedish Fracture Register: Evaluation of AO/OTA-classification in 152 ankle fractures. Injury, 2016; 47(11): 2579–83

19. Fischbach R, Prokop A, Maintz D et al: [Magnetic resonance tomography in the diagnosis of intra-articular tibial plateau fractures: Value of fracture classification and spectrum of fracture associated soft tissue injuries]. Rofo, 2000; 172(7): 597–603 [in German]

20. Needleman RL, Skrade DA, Stiehl JB: Effect of the syndesmotic screw on ankle motion. Foot Ankle, 1989; 10(1): 17–24

21. Hsu AR, Ellington JK: Patient-specific 3-Dimensional printed titanium truss cage with tibiotalocalcaneal arthrodesis for salvage of persistent distal tibia nonunion. Foot Ankle Spec, 2015; 8(6): 483–89

22. Chung KJ, Hong DY, Kim YT et al: Preshaping plates for minimally invasive fixation of calcaneal fractures using a real-size 3D-printed model as a preoperative and intraoperative tool. Foot Ankle Int, 2014; 35(11): 1231–36

23. Deshmukh TR, Kuthe AM, Vaibhav B: Preplanning and simulation of surgery using rapid modelling. J Med Eng Technol, 2010; 34(4): 291–94

24. Zheng W, Chen C, Zhang C et al: The feasibility of 3D printing technology on the treatment of pilon fracture and its effect on doctor-patient communication. Biomed Res Int, 2018; 2018: 8054698

25. Bai J, Wang Y, Zhang P et al: Efficacy and safety of 3D print-assisted surgery for the treatment of pilon fractures: A meta-analysis of randomized controlled trials. J Orthop Surg Res, 2018; 13(1): 283

26. Giannetti S, Bizzotto N, Stancati A, Santucci A: Minimally invasive fixation in tibial plateau fractures using an pre-operative and intra-operative real size 3D printing. Injury, 2017; 48(3): 784–88

27. Shams PN, Foster PJ: Clinical outcomes after lens extraction for visually significant cataract in eyes with primary angle closure. J Glaucoma, 2012; 21(8): 545–50

28. Bagaria V, Deshpande S, Rasalkar DD et al: Use of rapid prototyping and three-dimensional reconstruction modeling in the management of complex fractures. Eur J Radiol, 201; 80(3): 814–20

29. Hurson C, Tansey A, O'Donnchadha B et al: Rapid prototyping in the assessment, classification and preoperative planning of acetabular fractures. Injury, 2007; 38(10): 1158–62

30. Chen H, Wu D, Yang H, Guo K: Clinical use of 3D printing guide plate in posterior lumbar pedicle screw fixation. Med Sci Monit, 2015; 21: 3948–54

31. Wang X, Wei Z, Huang J et al: [Preliminary application of virtual preoperative reconstruction planning in pilon fractures]. Zhongguo Xiu Fu Chong Jian Wai Ke Za Zhi, 2016; 30(1): 44–49 [in Chinese]

32. Lou Y, Cai L, Wang C et al: Comparison of traditional surgery and surgery assisted by three dimensional printing technology in the treatment of tibial plateau fractures. Int Orthop, 2017; 41(9): 1875–80